Journal of Electrical Engineering and Automation (ISSN: 2582-3051)
www.irojournals.com/iroeea/

An Overall Improved Ant Colony Optimization algorithm trained BPNN for PV MPPT

Jia-bao Chang[1], Fang-lin Niu[2], Tao Chen[3]

[1]Department of Electronics and Communication Engineering, Liaoning University of Technology, China
[2]Associate Professor, Department of Electronics and Information Engineering, Liaoning University of Technology, China
[3]Department of Data Science and Big Data Technology, Liaoning University of Technology, China

E-mail: [1]920198501@qq.com

Abstract

A novel PV MPPT algorithm based on the overall improved ant colony optimization algorithm-trained BP neural network (OIACO-BPNN) has been proposed in this paper to overcome the poor prediction accuracy and slow convergence rate of the BP Neural Network (BPNN). Firstly, the pheromone updating model of the Ant Colony Optimization (ACO) algorithm is improved, and the weight coefficient is added to improve the convergence rate of the ACO algorithm. Secondly, the optimal weight threshold of BPNN is updated by Overall Improved Ant Colony Optimization (OIACO) algorithm. Thirdly, the optimized BPNN is employed to predict the Maximum Power Point (MPP) voltage of the photovoltaic (PV) array. Finally, the deviation value between the voltage of the PV array and the predicted voltage is employed as the input of PID controller. In addition, the duty cycle of the Boost circuit is adjusted by PID controller to achieve MPPT. Matlab/Simulink is employed to verify the feasibility and effectiveness of the proposed MPPT algorithm. Simulation results illustrate that the OIACO-BPNN algorithm is superior to the ACO and the BPNN in prediction accuracy and tracking performance, moreover has a good robustness and response speed.

Keywords: Ant colony optimization algorithm, BP neural network, MPPT, Photovoltaic power generation, Boost converter

1. Introduction

PV power generation has the characteristics of non-pollution and low cost. Hence, the PV power generation is widely promoted in the various countries. Photovoltaic modules have

DOI: https://doi.org/10.36548/jeea.2021.4.006
Received: 17.03.2022, received in revised form: 06.04.2022, accepted: 14.04.2022, published: 25.04.2022

strong nonlinearity and fluctuation, and the annual power generation is greatly affected by atmospheric conditions. Therefore, it is indispensable to research maximum power point algorithm (MPPT) [1-2].

Recently, researchers have proposed a variety of traditional MPPT and nature-inspired algorithm. The traditional MPPT algorithm includes Hill Climbing method, Perturb and Observe method (P&O), incremental conductance (INC), constant voltage tracking (CVT), adaptive P&O (AP&O) method. The traditional MPPT algorithm is the most widely used and has the characteristics of simplicity and easy implementation. Nature-inspired algorithm includes artificial neural networks (ANN), sparrow search algorithm (SSA), ACO, particle swarm optimization (PSO), whale optimization algorithm (WOA), beetle antennae search (BAS) algorithm. Although ANN has strong convergence speed and reasoning ability, it is prone to fall into local optimal. Based on the foraging behavior of birds. Eberhart and Kennedy proposed the PSO algorithm in 1995, the algorithm has fast convergence speed and strong searching ability, but it is prone to premature population. Compared with traditional MPPT algorithm, nature-inspired algorithm has higher tracking accuracy and can track the MPP faster [3-5].

In [6], a neural network-fuzzy control algorithm is proposed, first use neural network to predict the MPP voltage of PV modules, Then fuzzy control is used to control the duty cycle of Boost circuit to track the MPP of the PV array. In [7], Ye SP et al. introduced a hopping PSO algorithm, by reducing the number of particles in the duty cycle and shortening the tracking time, the tracking performance of MPPT algorithm has been improved. The authors of [8] have developed an adaptive conductance increment method with variable step size based on neural network optimization. By using the optimal scaling factor obtained by neural network, the step size of conductance increment method is adjusted to realize MPPT. In [9], an improved mayfly algorithm is proposed, the algorithm adopts double population cross search. The mayfly algorithm is employed to improve the stabilization accuracy and tracking speed under complex environment. In [10], Latifi, M et al. presented an improved P&O method of variable step size based on krill colony algorithm. Krill swarm algorithm is used to fine-tune the sliding mode reaching law, optimize the step size of disturbance observation method, and improve the efficiency of photovoltaic system. In [11], Yan, Z et al. introduced an adaptive fuzzy control MPPT algorithm, which using the dP/dU and D(n-1) to improve the optimization time and quickly track the MPP. The authors of [12] have

developed a novel statistical performance evaluation method, which can efficiently improve the response speed of the PV array.

To solve the above problems, a novel PV MPPT algorithm based on an overall improved ant colony optimization algorithm-trained BP neural network (OIACO-BPNN) algorithm is proposed in this dissertation. Firstly, the pheromone updating model of OIACO algorithm is improved Under different light intensity and temperature, the optimized BPNN is employed to predict the (MPP) voltage of PV array. Finally, the MPP voltage is tracked by PID controller and PWM technology.

The main contributions of our works are as follows:

1) This paper proposes an overall improved photovoltaic MPPT algorithm of ant colony optimization BPNN. By improving the pheromone model of ACO, the OIACO algorithm is adopted to update the weight threshold of BPNN.

2) The OIACO-BPNN algorithm has high tracking performance and stabilization accuracy as compared to ACO and the optimized BPNN under four automatic conditions.

The structure of this paper is organized as follows: PV array and Boost circuit is introduced in section 2. Related work including BPNN, ACO, OIACO and OIACO-BPNN algorithm are given in Section 3. Simulation results and discussion are given in section 4. Finally, the conclusion and future works are given in section 5.

2. Photovoltaic System

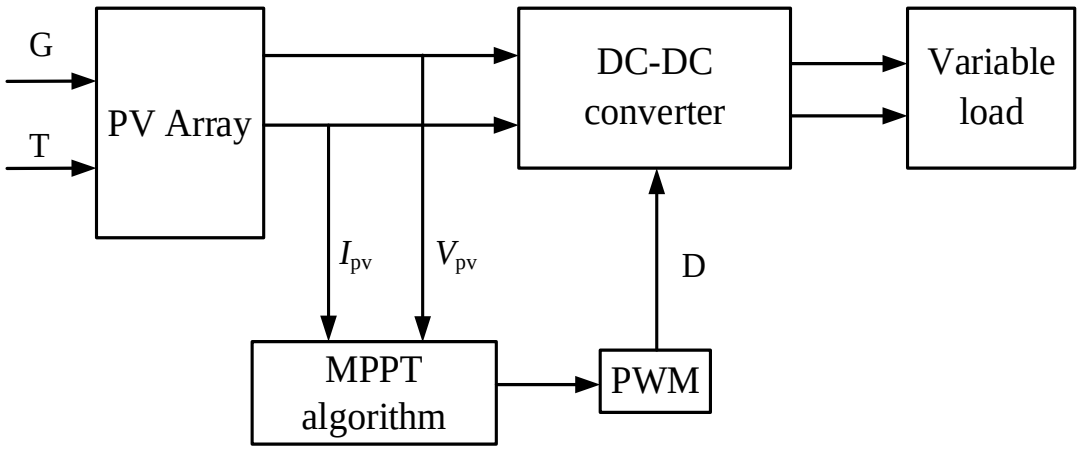

Figure 1. Photovoltaic power generation system structure

Photovoltaic power generation system is composed of PV array module, DC/DC conversion circuit, MPPT controller and variable load, The volt generation system is shown in Fig. 1. MPPT algorithm is employed to track the MPP of PV array to achieve load matching and make the PV array work near the MPP [6].

2.1 Mathematics Model of the PV Array

The single diode of PV array is shown in Fig. 2

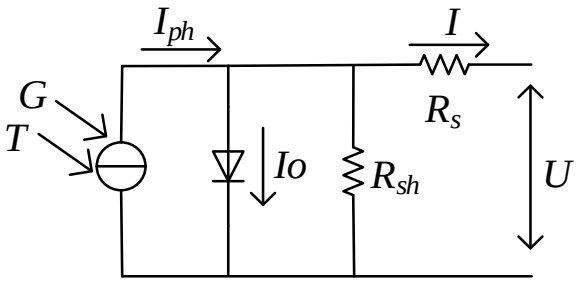

Figure 2. The single diode of PV array

The output current equation of PV array is given in Eq .(1).

$$I = I_{pv} - I_o\{\exp[\frac{q(U + R_s \times I)}{AKT}] - 1\} - \frac{U + R_s \times I}{R_{sh}} \quad (1)$$

Where I represents the output current of the PV array; U is the output voltage of the PV array; I_{pv} is the photocurrent; I_o is the saturation current; R_s is a series resistance, generally only a few ohms; R_{sh} is a shunt resistance, typically about a few thousand ohms; A is the ideal parameter of the diode, generally A is in the range of 1~2; K is Boltzmann constant, K=1.38×10-23 J/K; q is the charge parameter, q=1.6×10-19 C; T is the temperature of the PV array, expressed in ^oC [7].

PV array are simulated under different light intensity and temperature conditions, specific parameters are as follows: T=25 ^oC, the irradiations (G) are 200 W/m^2、400 W/m^2、600 W/m^2、800 W/m^2、1000 W/m^2、1200 W/m^2. The P-U-I characteristic curve of PV array is given in Fig. 3. As shown in Fig. 3, the MPP has no obvious drift with the irradiation, and short-circuit current and open-circuit voltage increase with the increase of light intensity [8-9]. G=1000 W/m^2, the temperatures are 20 ^oC, 25 ^oC, 35 ^oC and 45 ^oC. The output characteristic curve of PV array is shown in Fig. 4. It can be seen from Fig. 4 that as the temperature decreases, the maximum output power of the PV array gradually increases [10-11].

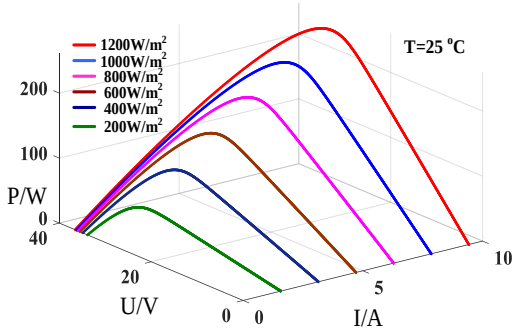

Figure 3. T=25°C, P-U-I output characteristic curve of PV array

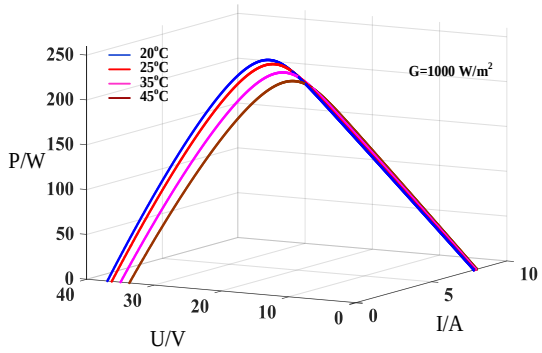

Figure 4. G=1000 W/m^2, P-U-I output characteristic curve of PV array

2.2 Boost Circuit

In PV power generation system, the function of MPPT is usually realized by DC/DC conversion circuit, Boost circuit has the characteristics of simple structure and high efficiency [12-14]. Boost circuit is adopted in this paper as the DC/DC conversion circuit in the PV power generation system, as shown in Fig. 5. The duty cycle D of the switch tube is adjusted to realize the transformation of the external load in real time. The resistance value of the external load is R, the voltage across the external load is U_o, and the current through the external load is I_o, then the equivalent load resistance R_s of the boost circuit is:

$$R_s = \frac{U_o(1-D)}{I_o(1-D)^{-1}} = R(1-D)^2 \tag{2}$$

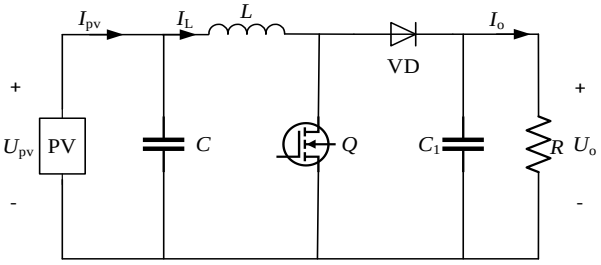

Figure 5. Boost circuit

3. PV Control Algorithm

3.1 BPNN Algorithm

BPNN is a global convergence network with good adaptability and generalization, and has been widely used in several fields. BPNN is compose of the input layer, hidden layer and output layer. The weight and threshold of the BPNN are set to the W_{ij} and B_n, respectively. The weight from the hidden layer to the output layer is set to W_{if}, and the threshold from the hidden layer to the output layer is set to b, The classical three-layer BPNN is shown in Fig. 6. The *L-M* function to adjust the weight threshold of the BPNN, and the weight threshold is updated by back propagation process.

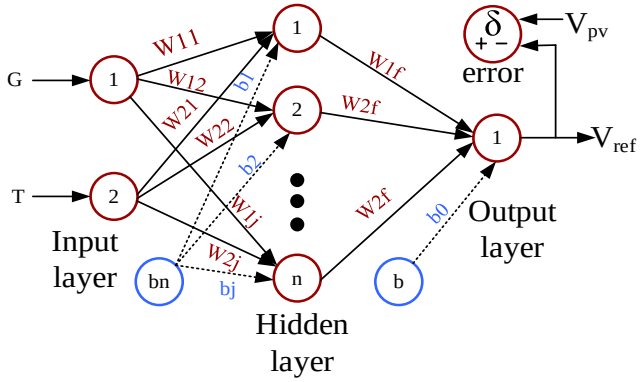

Figure 6. BPNN structure

The output layer equation of neural network is as follows:

$$\begin{aligned} V_{\text{ref}} &= f(net_{\text{i}}) \\ net_{\text{n}} &= \sum_{j=0}^{m} w_{\text{ij}} y_{\text{j}} \quad j = 1, 2, \cdots l \end{aligned} \tag{3}$$

The equation of the hidden layer is as follows:

$$\begin{aligned} y_{\text{j}} &= f(net_{\text{j}}) \qquad j = 1, 2, \cdots n \\ net_{\text{j}} &= \sum_{j=0}^{n} V_{\text{rf}} X_{\text{r}} \qquad j = 1, 2, \cdots n \end{aligned} \tag{4}$$

The fastest gradient descent method is employed to update the weight threshold of the BPNN. The updating equation is as follows:

$$W_{\text{ij}} = -\eta \frac{\partial J}{\partial W_{\text{ij}}} \quad i = 1, 2, \cdots l \quad j = 1, 2, \cdots n \tag{5}$$

$$b_{nj} = -\eta \frac{\partial J}{\partial b_i} \quad i = 1,2,\cdots l \quad j = 1,2,\cdots n \tag{6}$$

BPNN is essentially a gradient algorithm for nonlinear optimization problems. Due to the RBF neural network has slow convergence rate and weak performance, and the Euclidean norm will lead to a narrow center width. Moreover, the BP The algorithm cannot effectively learn and store a majority of mapping relationship and the value of the mean square error will cause the slow convergence rate. Therefore, the learning rate (η) play a particularly role in BPNN algorithm. The η determines the amount of change in the weights in each cycle. If the η is chosen too small, the adjustment of the weights becomes smaller each time and the network converges slowly. If the η is chosen too large, the adjustment of the weights becomes larger each time. A larger weight adjustment will led to the network to jump around the minimum error value, resulting in oscillations. and the network becomes divergent and cannot converge. Small η is adopted to ensure the stability of BPNN [15-18]. In the above equation, the η is an arbitrary value between [0,1]; J is the sum of squares of the difference between the real output and the calculated output, W_{ij} and B_{nj} are the weights and biases of the BPNN respectively. V_{ref} is the MPP voltage reference value.

3.2 ACO Algorithm

ACO is a bionic intelligent algorithm with excellent distributed computing mechanism and easy implementation. ACO originates from simulating the foraging behavior of ants. During the movement of the ant colony, pheromones are continuously secreted, and the ants can sense the pheromones and choose the foraging path with higher pheromone content. over time, the pheromone concentration on the short path accumulates, thus attracting more individuals to pass through the short path, and the final path with the highest pheromone concentration is the best path [19-23].

At each step of the path construction, the ant uses the roulette wheel algorithm to calculate the next position to be reached by the ant. The formula is shown in Eq. (7):

$$P_{ij}^{k} = \begin{cases} \dfrac{\tau_{ij}^{\alpha}(t) * \eta_{ij}^{\beta}(t)}{\sum_{s \in j_{k(i)}} \tau_{ij}^{\alpha}(t) * \eta_{ij}^{\beta}(t)} & j \in j_k(i) \\ 0 & other \end{cases} \tag{7}$$

Among them: i is the starting point; j is the end point; α is the pheromone factor; β is the heuristic function factor; $\tau_{ij}(t)$ denotes the pheromone concentration from i to j at time; $\eta_{ij}(t)=1/d_{ij}$ is the reciprocal of the distance path from point i to point j; Other denotes the set

of nodes that ant k has not reached; p_{ij}^{k} indicating the probability of ant k from point i to point j. According to the formula, the shorter the path, the higher the pheromone concentration, the higher the probability of path selection.

ACO can be divided into ant cycle model, ant-quantity model and ant-density model according to pheromone updating model. Ant-cycle model is a global updating mode in which all ants complete a path and update pheromones, ant-quantity model and ant-density model are local updating models in which ants update pheromones along the path after passing a node, The difference is that in the ant density model, the pheromone release of ants is constant, ant quantity model the pheromone concentration released by ants is related to the path traveled. Pheromone released by ants gradually volatilizes over time. After each ant passes the next node or passes all nodes, the relevant information and pheromone concentration left by ants need to be updated. Pheromone update formula is shown in Eq. (8).

$$\tau_{ij}(t+n)=(1-\rho)\ \tau_{ij}(t)+\sum_{k=1}^{m}\frac{Q}{L_k} \tag{8}$$

In the above formula, ρ is the pheromone volatile factor; Q is the pheromone quantity and quantity of an ant.

Ant colony algorithm steps:

1. Initialize the parameters (ant number m, pheromone factor α, pheromone constant Q, iteration times t and more).

2. Construct the searching space, the populations are randomly set at different positions, and calculate the k of each ant (k=1,2,3... M) next node until all of the ant colony have reached all of nodes.

3. The pheromone of ant is updated to calculate the path length of each ant L_k (k=1,2... , m). In addition, the optimal solution (shortest path) is recorded in the current iteration number. Moreover, the pheromone concentration of the ant colony is updated.

4. Determine whether to terminate or not. If the termination condition is not met, return to step (2); otherwise, the optimal solution is output. Fig. 7 is the ACO process diagram.

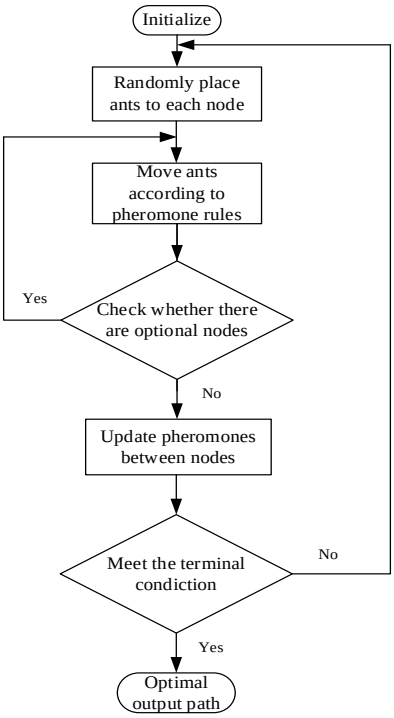

Figure 7. ACO process

3.3 OIACO Algorithm

Since the conventional ACO algorithm has the slow convergence rate and the population is prone to prematurity, an overall improved ant colony optimization is proposed in the dissertation. Average fitness (f_{avg}) is compared with current fitness (f), If f is greater than f_{avg}, the pheromone volatility coefficient ρ is diluted [24-25], otherwise, the current pheromone concentration is retained to avoid the premature convergence of the algorithm into the local optimal solution. The adaptive adjustment of ρ value is shown in Eq. (9). The weight coefficient of pheromone update formula was added to the index to improve the convergence speed and accuracy of the algorithm. The pheromone update formula of OIACO is shown in Eq. (10). The error of the algorithm is the average value of the *MSE* function test set and training set, as shown in Eq. (11).

$$\begin{cases} \rho_{t+1} = \rho_t \; f \le f_{avg} \\ \rho_{t+1} = 0.95\rho_t \; f \ge f_{avg} \end{cases} \tag{9}$$

$$\Delta \tau_{ij} = \sum_{k=1}^{w} (1-\rho)\Delta \tau_{ij}^{k} + e^{-t}\Delta \tau_{ij} \tag{10}$$

$$LOSS = \frac{MSE_{(train)} + MSE_{(test)}}{2} \tag{11}$$

3.4 OIACO-BPNN Algorithm

The algorithm proposed in this paper is a fusion of OIACO and BPNN, Through the global random search algorithm of ACO, BPNN is trained to generate a set of optimal weight threshold value, which improves the convergence speed of BPNN and reduces the risk of falling into local optimal solution. The flow chart of OIACO-BPNN algorithm proposed in this paper is shown in Fig. 8.

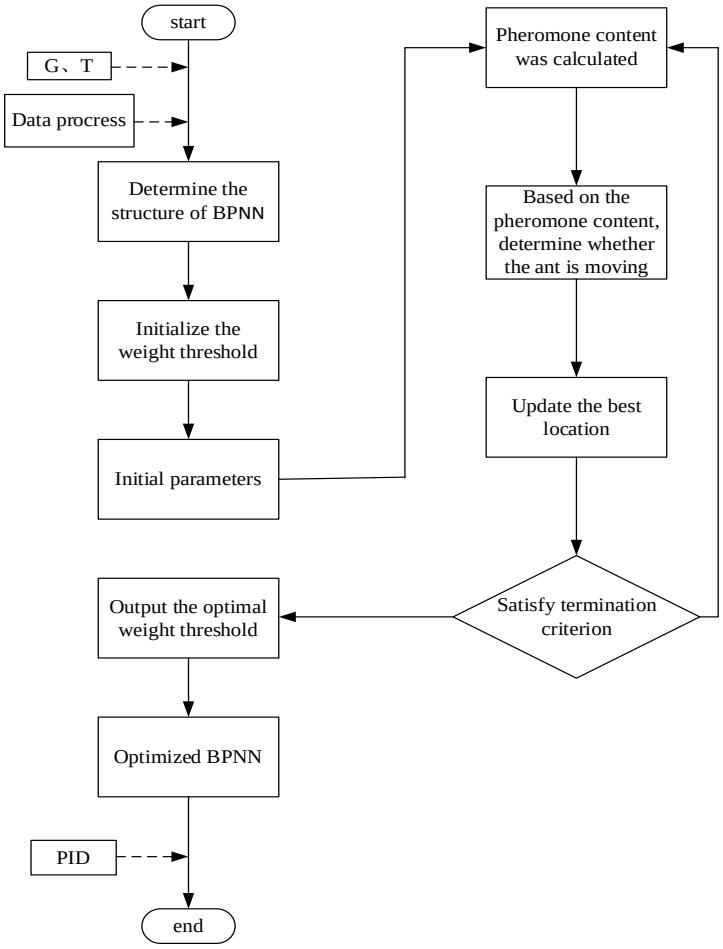

Figure 8. OIACO-BPNN algorithm process

The specific steps of OIACO-BPNN algorithm are shown below:

1) Sampling light intensity and temperature as data sets, and determining the structure of BPNN.

2) The number of ants m, pheromone volatile factor ρ, pheromone constant Q, the maximum number of iterations t are initialized by calculating the dimensions of the solution space.

3) The pheromone content was calculated according to the position of the ant. Calculate the maximum pheromone and update the optimal individual location. Probabilistically transfer and update ant positions. Update according to formula (8).

4) Step (3) is repeated. After the termination iteration number is reached, the optimal ant position coordinates after optimization are taken out and assigned to the BPNN to obtain the optimal initial weight matrix and threshold vector.

5) The optimized BPNN is trained and tested to predict the MPP voltage.

6) PID controller and PWM technology are used to control the on-off time of Boost circuit.

Fig. 9 shows the error comparison between the optimized BPNN and the traditional BPNN. The error of BPNN is within the range is within [-0.001, 0.001], and the error of BPNN optimized by overall improved ant colony optimization algorithm is within the range is within [-0.00005,0.00005]. Simulation results show that the prediction accuracy of the optimized BPNN has been greatly improved.

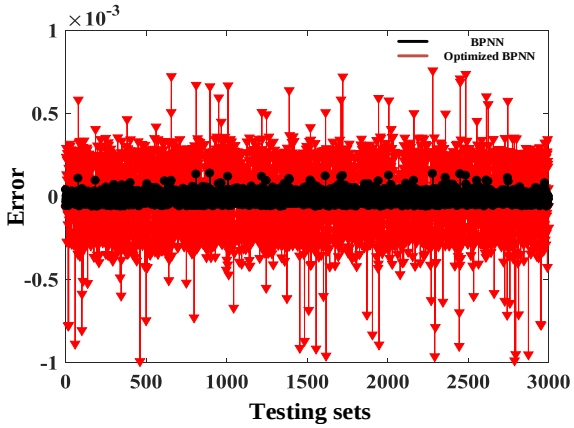

Figure 9. The best performance of the conventional BPNN and the optimized BPNN

4. Simulation results and analysis

To verify the feasibility of the proposed MPPT algorithm, four conditions (standard condition, slow change of illumination, sudden change of illumination, continuous change of temperature), the tracking results of the MPP of the improved OIACO-BPNN algorithm, ACO and BPNN algorithm are simulated, and the control performance of the three algorithms is analyzed.

4.1 Data Set

Matlab is employed to obtain the input and output datasets, the input is the irradiation and temperature, the output is the MPP voltage (V_{mpp}). The inputs and output datasets are obtained by 10,000 cycles of Eqs. (18), (19) and (20). 70% of the datasets are the training sets and 30% of the datasets are the testing sets.

$$G = (G_{max} - G_{min})rand + G_{min} \tag{12}$$

$$T = (T_{max} - T_{min})rand + T_{min} \tag{13}$$

$$V_{mpp} = V_{mps} + (beta(T - T_{ref}) \tag{14}$$

Where the G_{max} is 1200 W/m^2, G_{min}= 0 W/m^2; T_{max}=60 ^{o}C, T_{min}=0 ^{o}C, rand is a random value in [0,1]; V_{mps} is the MPP voltage of the PV array under standard test condition (G_{ref}=1000 W/m^2, T_{ref}=25 ^{o}C); beta is the temperature coefficient.

4.2 Simulation circuit model

The Boost circuit of PV system is constructed in simulink/Matlab, as shown in Fig 10. Implementation of MPPT algorithm by OIACO-BPNN algorithm, compared with BPNN, OIACO algorithm under different conditions. The final result of OIACO-BPNN is better. The simulation time duration is 2s and the simulation algorithm is ode23 (Bogacki-Shampine).

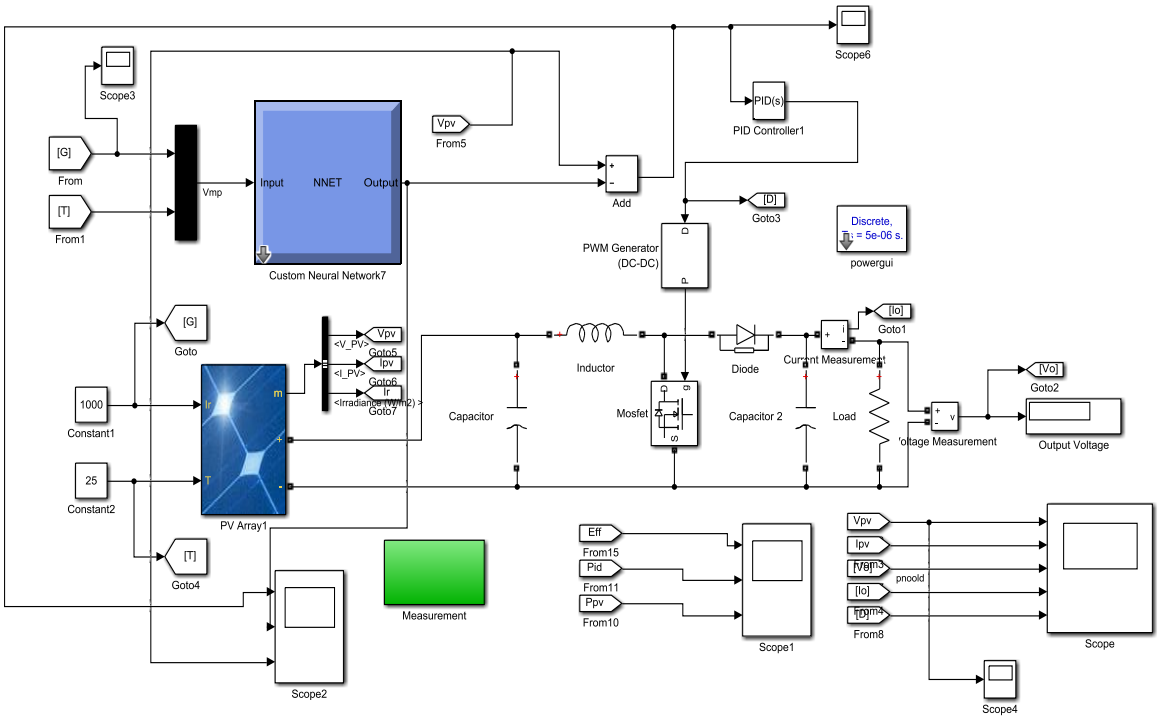

Figure 10. Simulation circuit model

4.3 MPPT curve under Standard test Condition

Fig 11 shows the output power waveform under standard conditions, it can be seen from Fig. 11. In the start-up stage, the tracking speed of OIACO-BPNN algorithm is 0.002 s, compared with the ACO algorithm and BPNN algorithm, which are 0.006 s and 0.008 s respectively. OIACO-BPNN algorithm can reach the MPP faster. When the maximum power tracking of the three algorithms reaches the stable state, the oscillation of OIACO-BPNN algorithm is minimum and stable output.

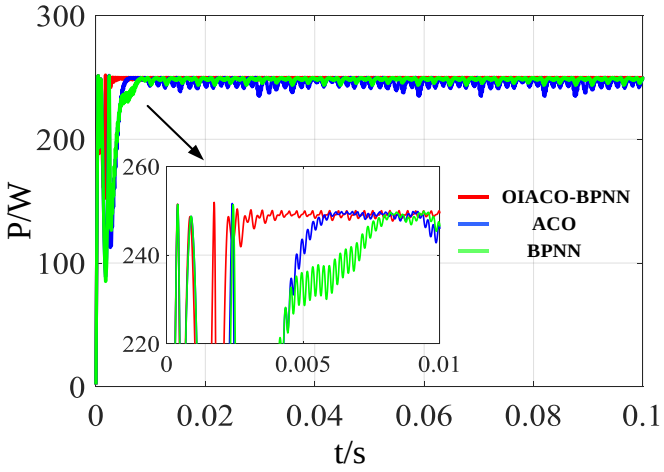

Figure 11. Output power waveform in standard condition

4.4 Light Changes Slowly

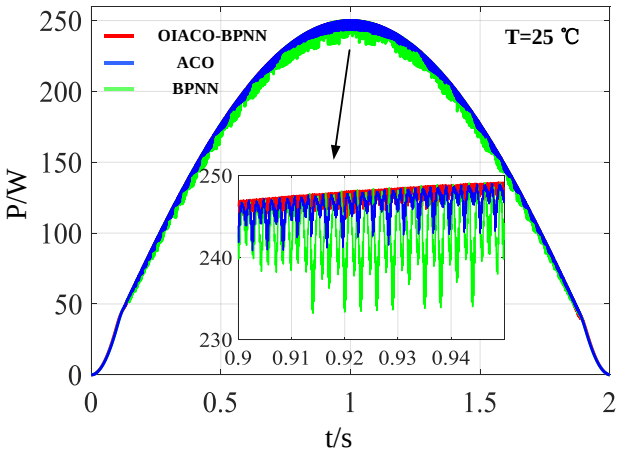

Figure 12. Illumination slowly changes the output power waveform

To simulate the change of light intensity from morning to dusk, the light intensity parameters are as follows: T=25 oC, T= 0 s, G=0 W/m2; When t=1 s, the peak point G=1000 W/m2. When t=2 s, G=0 W/m2, Fig. 12 shows the output power waveform of light slowly

changing. As shown in Fig. 12, when the irradiation rises slowly, the maximum output power of PV array increases, t=1 s, and the output power and light intensity reach the peak point at the same time. The chattering of the maximum tracking power curve of OIACO-BPNN is significantly smaller than that of the ACO algorithm and the BPNN algorithm.

4.5 Sudden Change of Light

PV modules are nonlinear, and the efficiency of PV system is greatly affected by illumination. The illumination variation parameters are as follows: at the startup, the irradiation is 500 W/m^2; at t=0.5 s, the illumination intensity changes from 500 W/m^2 to 1000 W/m^2, and the maximum power of PV array increases from 130 W to 250 W. The OIACO-BPNN algorithm has smaller oscillation amplitude and faster tracking speed during the sudden change of illumination.

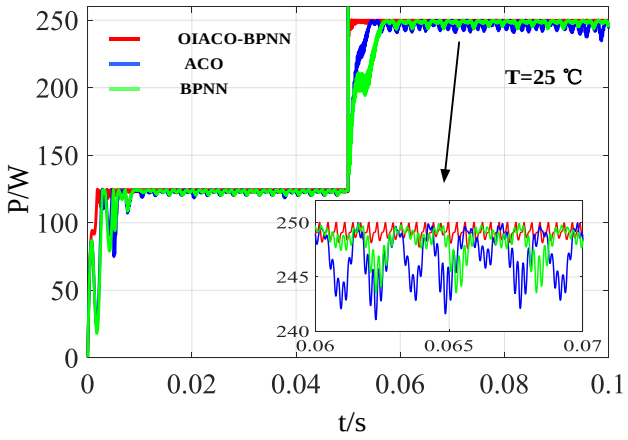

Figure 13. Light abrupt output power waveform on sudden change of light

4.6 Continuous Temperature Change

Rain and snow weather will lead to continuous temperature changes, and the temperature parameters are as follows: 0 s-0.6 s, T=20 ℃; 0.6 s-0.11 s, T suddenly increases to 50 ℃; At 0.11 s-0.15 s, T suddenly decreases to 25 ℃, and the output power waveform with continuous temperature change is shown in Fig. 14. Simulation results show that ACO algorithm and BPNN algorithm reach the MPP at 0.006 s and 0.008 s respectively in the start-up stage, while OIACO-BPNN algorithm reaches the MPP at 0.003 s, which is obviously faster than the other two algorithms. When the temperature of 0.6 s suddenly rises to 50 ℃, the maximum output power decreases from 255 W to 245 W, and when the temperature of 0.11 s drops to 25 ℃, the maximum output power increases to 250 W. In the process of continuous temperature change, the accuracy of OIACO-BPNN algorithm is high.

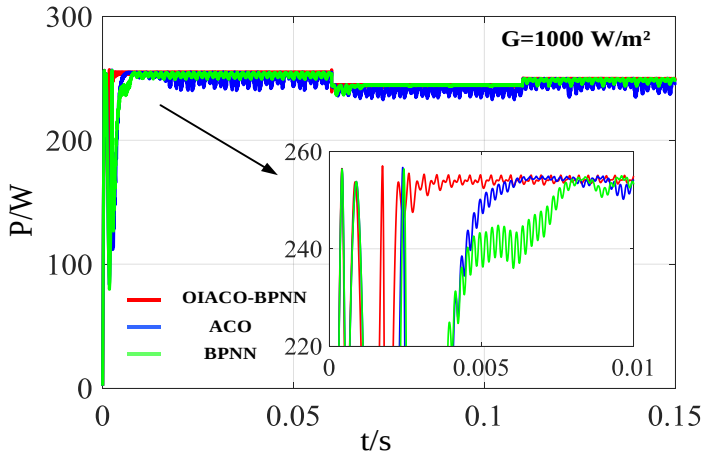

Figure 14. Light abrupt output power waveform on continuous temperature change

According to the analysis of appeal, the proposed OIACO-BPNN algorithm can quickly reach the stable state under the change of temperature or the change of light intensity. After reaching the stable state, the power fluctuation is minimized, and it has good steady-state accuracy.

5. Conclusion

This paper proposes a novel PV MPPT algorithm based on the overall improved ant colony optimization algorithm-trained BP neural network. Initially the pheromone updating model of the ACO algorithm is improved for enhancing the convergence rate of the ACO algorithm and then the optimized weight threshold of BPNN is updated by OIACO algorithm. Next, the optimized BPNN is employed to predict the MPP voltage of the PV array and at last the MPP voltage is tracked by PID controller and PWM technology. The result shows that the OIACO has good global optimization and the BPNN has strong adaptability and fault tolerance. The OIACO-BPNN algorithm is compared with ACO algorithm and BPNN under four conditions (standard test condition, slow illumination change, illumination mutation and continuous temperature change). Experimental results demonstrate that the OIACO-BPNN algorithm has better tracking performance, adaptability, and stability than the two compared algorithms.

References

[1] Babes, B., Boutaghane, A., Hamouda, N. (2022). A novel nature-inspired maximum power point tracking (MPPT) controller based on ACO-ANN algorithm for

photovoltaic (PV) system fed arc welding machines. Neural Computing and Applications, 34(1), 299-317.

[2] Javed, S., Ishaque, K. (2022). A comprehensive analyses with new findings of different PSO variants for MPPT problem under partial shading. Ain Shams Engineering Journal, 13(5), 101680.

[3] Haseeb, I., Armghan, A., Khan, W., Alenezi, F., Alnaim, N., Ali, F., Ullah, N. (2021). Solar Power System Assessments Using ANN and Hybrid Boost Converter Based MPPT Algorithm. Applied Sciences, 11(23), 11332.

[4] Abdali, A., & Mazlumi, K. (2021). AC/DC robust controller technique for reliable operation of photovoltaic-based microgrid using firefly algorithm and fuzzy logic. International Journal of Emerging Electric Power Systems, 22(4), 451-462.

[5] Kavya, M., Jayalalitha, S. (2022). A novel coarse and fine control algorithm to improve Maximum Power Point Tracking (MPPT) efficiency in photovoltaic system. ISA transactions, 121, 180-190.

[6] Ali, M. N., Mahmoud, K., Lehtonen, M., Darwish, M. M. (2021). Promising MPPT Methods Combining Metaheuristic, Fuzzy-Logic and ANN Techniques for Grid-Connected Photovoltaic. Sensors, 21(4), 1244.

[7] Ji, B., Hata, K., Imura, T., Hori, Y., Honda, S., Shimada, S., Kawasaki, O. (2020). A Novel Particle Jump Particle Swarm Optimization Method for PV MPPT Control under Partial Shading Conditions. IEEJ Journal of Industry Applications, 9(4), 435-443.

[8] Ye, S. P., Liu, Y. H., Liu, C. Y., Ho, K. C., Luo, Y. F. (2021). Artificial Neural Network Assisted Variable Step Size Incremental Conductance MPPT Method with Adaptive Scaling Factor. Electronics, 11(1), 43.

[9] Mo, S., Ye, Q., Jiang, K., Mo, X., Shen, G. (2022). An improved MPPT method for photovoltaic systems based on mayfly optimization algorithm. Energy Reports, 8, 141-150.

[10] Latifi, M., Abbassi, R., Jerbi, H., Ohshima, K. (2021). Improved krill herd algorithm based sliding mode MPPT controller for variable step size P&O method in PV system under simultaneous change of irradiance and temperature. Journal of the Franklin Institute, 358(7), 3491-3511.

[11] Yan, Z., Ya-Jun, W. Jia-Bao, C. (2021). A Novel Adaptive Fuzzy MPPT Algorithm under Changing Atmospheric Conditions. Journal of Electrical Engineering and Automation, 3(4), 246-264.

[12] Rezk, H., Mazen, A. O., Gomaa, M. R., Tolba, M. A., Fathy, A., Abdelkareem, M. A., Abou Hashema, M. (2019). A novel statistical performance evaluation of most modern optimization-based global MPPT techniques for partially shaded PV system. Renewable and Sustainable Energy Reviews, 115, 109372.

[13] He, X., He, B., Zhao, Y., Cui, R., Zhang, J., Dong, Y., Jiang, R. (2021). MPPT control based on improved mayfly optimization algorithm under complex shading conditions. International Journal of Emerging Electric Power Systems, 22(6), 661-674.

[14] Sarwar, S., Hafeez, M. A., Javed, M. Y., Asghar, A. B., Ejsmont, K. (2022). A Horse Herd Optimization Algorithm (HOA)-Based MPPT Technique under Partial and Complex Partial Shading Conditions. Energies, 15(5), 1880.

[15] Mohammed, S. S., Devaraj, D., Ahamed, T. P. (2021). GA-Optimized Fuzzy-Based MPPT Technique for Abruptly Varying Environmental Conditions. Journal of The Institution of Engineers (India): Series B, 102(3), 497-508.

[16] An, Q., Tang, R., Su, H., Zhang, J., Li, X. (2021). Robust configuration and intelligent MPPT control for building integrated photovoltaic system based on extreme learning machine. Journal of Intelligent & Fuzzy Systems, (Preprint), 1-18.

[17] Villegas-Mier, C. G., Rodriguez-Resendiz, J., Álvarez-Alvarado, J. M., Rodriguez-Resendiz, H., Herrera-Navarro, A. M., Rodríguez-Abreo, O. (2021). Artificial neural networks in MPPT algorithms for optimization of photovoltaic power systems: A review. Micromachines, 12(10), 1260.

[18] Fathi, M., Parian, J. A. (2021). Intelligent MPPT for photovoltaic panels using a novel fuzzy logic and artificial neural networks based on evolutionary algorithms. Energy Reports, 7, 1338-1348.

[19] Wani, T. A. (2021). A Review of Fuzzy Logic and Artificial Neural Network Technologies Used for MPPT. Turkish Journal of Computer and Mathematics Education (TURCOMAT), 12(2), 2912-2918.

[20] Haq, I. U., Khan, Q., Ullah, S., Khan, S. A., Akmeliawati, R., Khan, M. A., Iqbal, J. (2022). Neural network-based adaptive global sliding mode MPPT controller design for stand-alone photovoltaic systems. Plos one, 17(1), e0260480.

[21] Abdelaziz, Z., Ahmed, M., Khadidja, B., Djamila, R., Adel, O., Eddine, M. N. (2021). Enhancement of Extracted Photovoltaic Power Using Artificial Neural Networks MPPT Controller. In Advances in Green Energies and Materials Technology (pp. 265-272). Springer, Singapore.

[22] Zafar, M. H., Khan, N. M., Mirza, A. F., Mansoor, M., Akhtar, N., Qadir, M. U., Moosavi, S. K. R. (2021). A novel meta-heuristic optimization algorithm based MPPT control technique for PV systems under complex partial shading condition. Sustainable Energy Technologies and Assessments, 47, 101367.

[23] Laxman, B., Annamraju, A., Srikanth, N. V. (2021). A grey wolf optimized fuzzy logic based MPPT for shaded solar photovoltaic systems in microgrids. International Journal of Hydrogen Energy, 46(18), 10653-10665.

[24] Chao, K. H., Rizal, M. N. (2021). A hybrid MPPT controller based on the genetic algorithm and ant colony optimization for photovoltaic systems under partially shaded conditions. Energies, 14(10), 2902.

[25] Aly, M., Rezk, H. (2021). A MPPT based on optimized FLC using manta ray foraging optimization algorithm for thermo-electric generation systems. International Journal of Energy Research, 45(9), 13897-13910.

Author's biography

Jia-bao Chang completed his bachelor degree in Communication Engineering and doing his masters majoring in Electronic and Communication Engineering, in Liaoning University of Technology, He is currently researching technologies related to photovoltaic power generation systems.

Fang-lin Niu is an Associate professor of Liaoning University of technology, China, graduated from Dalian University of technology with a doctor's degree, mainly engaged in the research of electronic information technology and power electronics technology.

Tao Chen is an undergraduate student, majoring in Data Science and Big Data Technology in Liaoning University of Technology, China.